

Performance Analysis of OTFS Modulation with Transmit Antenna Selection

Vighnesh S Bhat and A. Chockalingam

Department of ECE, Indian Institute of Science, Bangalore 560012

Abstract—In this paper, we consider transmit antenna selection (TAS) in orthogonal time frequency space (OTFS) modulation and analyze its performance. We assume that the channel is quasi-static in the delay-Doppler (DD) domain and there is limited feedback from the receiver to the transmitter. The diversity performance of TAS is analyzed in a multiple-input multiple-output OTFS (MIMO-OTFS) system. Antenna selection is done based on the maximum channel Frobenius norm in the DD domain, where n_s antennas are selected out of n_t transmit antennas. Our analysis for one resolvable path in the DD channel (i.e., $P = 1$) shows that *i*) when $n_s = 1$, full spatial diversity of $n_r n_t$ (i.e., full receive diversity of n_r and full transmit diversity of n_t) is achieved since the underlying symbol difference matrix is full rank, and *ii*) when $n_s > 1$, only n_r th order receive diversity is achieved because of rank deficiency. Simulation results are shown to validate the analytically predicted diversity performance. For $P > 1$, diversity orders are predicted through rank of the difference matrices, validated through computation of pairwise error probability (PEP) bounds and simulations.

keywords: OTFS modulation, MIMO-OTFS, transmit antenna selection, spatial diversity, DD diversity.

I. INTRODUCTION

Next generation wireless communication systems beyond 5G are envisaged to operate in high-mobility/Doppler scenarios such as V2X communications, high-speed trains, and mm-wave communications. These systems should be capable of supporting high data rates and reliability in rapidly time-varying channels. Orthogonal time frequency space (OTFS) modulation is a novel modulation scheme proposed in recent literature to tackle the doubly-dispersive nature of high-Doppler channels [1],[2]. This modulation scheme multiplexes information symbols in the DD domain, unlike conventional multicarrier modulation schemes (e.g., OFDM), which use the time-frequency (TF) domain. The multiplexed symbols in the DD domain undergo 2D circular convolution with the channel in DD, such that each symbol encounters almost constant channel gain even in the rapidly time-varying channels. Because of the constant DD channel gain experienced by the symbols, channel estimation and equalization overhead is reduced. One more advantage of OTFS modulation is that it can be implemented using existing multicarrier architectures such as OFDM with additional pre- and post-processing blocks.

Several recent articles on the OTFS modulation have addressed key issues such as channel estimation [3]-[4], low-complexity signal detection [5]-[7], multiple access [8]-[10],

peak-to-average power ratio (PAPR), and pulse shaping [11]-[12]. Asymptotic diversity analysis of OTFS is carried out in [13] and it has been shown that the asymptotic diversity of single-input single-output OTFS (SISO-OTFS) is one. It also explored a phase rotation scheme to extract full DD diversity. It established the diversity orders of MIMO-OTFS with phase rotation and without phase rotation, which are $n_r P$ and n_r respectively, where n_r is the number of receive antennas and P is the number of resolvable paths in the DD channel. Space-time coded OTFS (STC-OTFS) is proposed in [14], where it exploits the Alamouti structure generalized to matrices to achieve full transmit diversity.

Practical MIMO systems have cost and complexity issues. Antenna selection is an effective solution to address the RF hardware complexity issue without compromising much in performance. Antenna selection at the transmitter can reduce the number of transmit radio frequency (RF) chains. Also, the diversity performance of OTFS with transmit antenna selection (TAS) has not been reported so far. Motivated by the above observations, our contribution in this paper is the analysis of the diversity performance of OTFS in the presence of antenna selection at the transmitter. We assume the channel is quasi-static in the DD domain and there is limited feedback from the receiver to the transmitter. The antennas are selected based on the channel Frobenius norms of the transmit antennas in the DD domain. Our performance analysis in this paper establishes the diversity achieved by the MIMO-OTFS system with antenna selection at the transmitter. When the number resolvable paths in the DD channel is one ($P = 1$), our analysis shows full spatial diversity is achieved for a full rank MIMO-OTFS and only receive diversity is achieved for a rank deficient MIMO-OTFS system with antenna selection at the transmitter. Simulation results are presented to validate the analytical results. For $P > 1$, diversity performance is obtained through the rank of the symbol difference matrices, validated through pairwise error probability (PEP) bounds and simulations. The performance MIMO-OTFS with Frobenius norm based selection is compared with random antenna selection and without antenna selection to demonstrate the diversity achieved by the Frobenius norm based selection.

The paper is organized as follows. The system model for MIMO-OTFS with TAS is presented in Sec. II. Diversity analyses are presented in Sec. III. Results and discussions are presented in Sec. IV. Conclusions are presented in Sec. V.

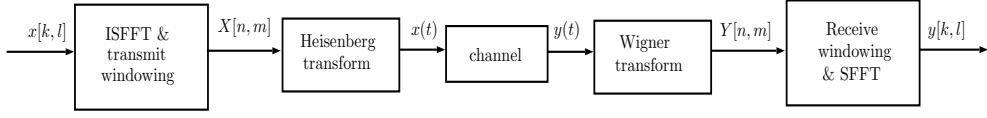


Fig. 1: OTFS modulation scheme.

II. SYSTEM MODEL FOR MIMO-OTFS WITH TAS

In this section, we introduce the system model. Towards this, we present the input-output relation of basic OTFS modulation and its extension to MIMO-OTFS with TAS.

A. Basic OTFS modulation

Consider the basic OTFS system which transmits and receives QAM/PSK information symbols. Figure 1 shows the basic OTFS modulation scheme. It consists of cascade structures of 2D transforms both at transmitter and receiver. It can also be viewed as a conventional OFDM system with additional pre- and post-processing modules at the transmitter and receiver. At the transmitter, the information symbols in the DD domain are transformed to TF domain through 2D inverse symplectic finite Fourier transform (ISFFT) followed by windowing. Using Heisenberg transform, the TF domain signal is transformed to time domain for transmission over the wireless channel. At the receiver, Wigner transform and 2D symplectic finite Fourier transform (SFFT) are performed to get the symbols in DD domain for demodulation.

The information symbols $x[k, l]$ s are arranged in 2D $N \times M$ DD grid, given by

$$\Upsilon = \left\{ \left(\frac{k}{NT}, \frac{l}{M\Delta f} \right), k = 0, \dots, N-1, l = 0, \dots, M-1 \right\}, \quad (1)$$

where $1/NT$ and $1/M\Delta f$ are the Doppler resolution and delay resolution, respectively, and N and M are the number of Doppler bins and delay bins, respectively. The information symbols $x[k, l]$ in the DD domain are mapped to the TF domain using ISFFT. Assuming rectangular windowing, the TF signal can be written as

$$X[n, m] = \frac{1}{\sqrt{MN}} \sum_{k=0}^{N-1} \sum_{l=0}^{M-1} x[k, l] e^{j2\pi \left(\frac{nk}{N} - \frac{ml}{M} \right)}. \quad (2)$$

The TF signal $X[n, m]$ is transformed to a time domain signal $x(t)$, using Heisenberg transform and transmit pulse $g_{tx}(t)$, as

$$x(t) = \sum_{n=0}^{N-1} \sum_{m=0}^{M-1} X[n, m] g_{tx}(t - nT) e^{j2\pi m \Delta f (t - nT)}. \quad (3)$$

The signal $x(t)$ transmitted through the channel, whose complex baseband channel response can be modeled in the DD domain as

$$h(\tau, \nu) = \sum_{i=1}^P h_i \delta(\tau - \tau_i) \delta(\nu - \nu_i), \quad (4)$$

where P is the number of paths in the DD domain, and h_i , τ_i , and ν_i are the channel gain, delay, and Doppler shift of the

i th path, respectively. The received time domain signal $y(t)$ can be expressed as

$$y(t) = \int_{\nu} \int_{\tau} h(\tau, \nu) x(t - \tau) e^{j2\pi \nu (t - \tau)} d\tau d\nu + v(t), \quad (5)$$

where $v(t)$ is the additive white Gaussian noise. At the receiver, Wigner transform is performed on the received signal $y(t)$ to get the TF domain signal $Y[n, m]$, as

$$Y[n, m] = \left[\int g_{rx}^*(t' - t) y(t') e^{-j2\pi f(t' - t)} dt' \right]_{t=nT, f=m\Delta f}, \quad (6)$$

where $g_{rx}(t)$ is the receive pulse. The pulses $g_{tx}(t)$ and $g_{rx}(t)$ are chosen in order to satisfy bi-orthogonality condition. Using SFFT, the TF signal is mapped to the DD domain signal as

$$y[k, l] = \frac{1}{\sqrt{MN}} \sum_{k=0}^{N-1} \sum_{l=0}^{M-1} Y[n, m] e^{-j2\pi \left(\frac{nk}{N} - \frac{ml}{M} \right)}. \quad (7)$$

Using (3)-(7), the input-output relation in the DD domain can be written as [5]

$$y[k, l] = \sum_{i=1}^P h'_i x[(k - \beta_i)_N, (l - \alpha_i)_M] + v[k, l], \quad (8)$$

where $h'_i = h_i e^{-j2\pi \nu_i \tau_i}$, α_i and β_i are assumed to be integers satisfying $\tau_i \triangleq \frac{\alpha_i}{M\Delta f}$ and $\nu_i \triangleq \frac{\beta_i}{NT}$, $(\cdot)_N$ denotes the modulo N operation, and $v[k, l]$ denotes the additive white Gaussian noise. Here, h_i s are assumed to be i.i.d and are distributed as $\mathcal{CN}(0, 1/P)$ with uniform scattering profile. The input-output in (8) can be vectorized as [5]

$$\mathbf{y} = \mathbf{H}\mathbf{x} + \mathbf{v}, \quad (9)$$

where $\mathbf{H} \in \mathbb{C}^{MN \times MN}$, $\mathbf{x}, \mathbf{y}, \mathbf{v} \in \mathbb{C}^{MN \times 1}$, the $(k + Nl)$ th entry of \mathbf{x} , $x_{k+Nl} = x[k, l]$, $k = 0, \dots, N-1, l = 0, \dots, M-1$, and $x[k, l] \in \mathbb{S}$, where \mathbb{S} is the modulation alphabet (e.g., QAM/PSK). Similarly, $y_{k+Nl} = y[k, l]$ and $v_{k+Nl} = v[k, l]$, $k = 0, \dots, N-1, l = 0, \dots, M-1$.

An alternate input-output relation for (9): The input-output relation in (9) can be written in an alternate form for diversity analysis. We observe that there are only P non-zero entries in each row and each column of the equivalent channel matrix \mathbf{H} because of modulo operation. Hence, (9) can be written in an alternate form as

$$\mathbf{y}^T = \mathbf{h}'\mathbf{X} + \mathbf{v}^T, \quad (10)$$

where \mathbf{y}^T is $1 \times MN$ received signal vector, \mathbf{h}' is $1 \times P$ channel vector whose i th entry is given by $h'_i = h_i e^{-j2\pi \nu_i \tau_i}$, \mathbf{v}^T is $1 \times MN$ noise vector, and \mathbf{X} is $P \times MN$ signal matrix

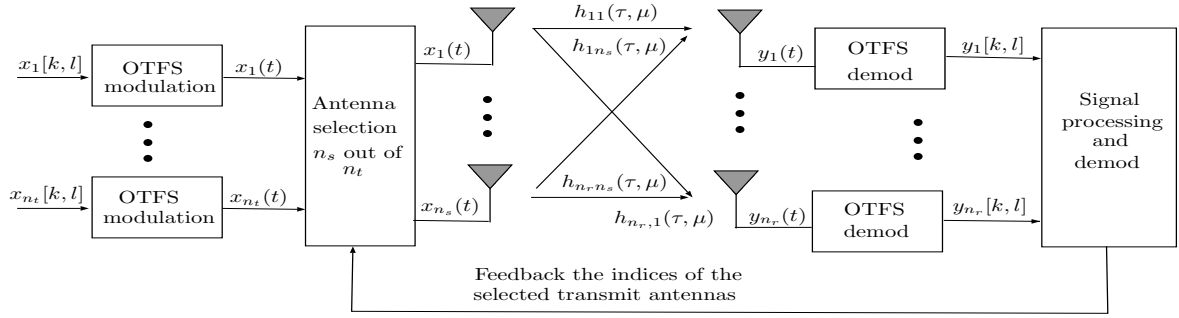


Fig. 2: MIMO-OTFS with transmit antenna selection.

whose i th column $\mathbf{X}[i]$, $i = k + Nl$, $k = 0, \dots, N - 1$, $l = 0, \dots, M - 1$, is given by

$$\mathbf{X}[i] = \begin{bmatrix} x_{(k-\beta_1)N+N(l-\alpha_1)M} \\ x_{(k-\beta_2)N+N(l-\alpha_2)M} \\ \vdots \\ x_{(k-\beta_P)N+N(l-\alpha_P)M} \end{bmatrix}. \quad (11)$$

This representation is useful for diversity analysis.

B. MIMO-OTFS with TAS

Following (9), the input-output relation of MIMO-OTFS system with n_r receive antennas and n_t transmit antennas can be written as

$$\underbrace{\begin{bmatrix} \mathbf{y}_1 \\ \vdots \\ \mathbf{y}_{n_r} \end{bmatrix}}_{\triangleq \bar{\mathbf{y}}} = \underbrace{\begin{bmatrix} \mathbf{H}_{11} & \cdots & \mathbf{H}_{1n_t} \\ \vdots & \ddots & \vdots \\ \mathbf{H}_{n_r1} & \cdots & \mathbf{H}_{n_r n_t} \end{bmatrix}}_{\triangleq \bar{\mathbf{H}}} \underbrace{\begin{bmatrix} \mathbf{x}_1 \\ \vdots \\ \mathbf{x}_{n_t} \end{bmatrix}}_{\triangleq \bar{\mathbf{x}}} + \underbrace{\begin{bmatrix} \mathbf{v}_1 \\ \vdots \\ \mathbf{v}_{n_r} \end{bmatrix}}_{\triangleq \bar{\mathbf{v}}}, \quad (12)$$

or equivalently

$$\bar{\mathbf{y}} = \bar{\mathbf{H}}\bar{\mathbf{x}} + \bar{\mathbf{v}}, \quad (13)$$

where $\bar{\mathbf{y}} \in \mathbb{C}^{n_r MN \times 1}$ is received signal vector, $\bar{\mathbf{H}} \in \mathbb{C}^{n_r MN \times n_t MN}$ is the overall equivalent channel matrix with \mathbf{H}_{ij} being the $MN \times MN$ equivalent channel matrix between the j th transmit antenna and i th receive antenna, $\bar{\mathbf{x}} \in \mathbb{C}^{n_t MN \times 1}$ is the OTFS transmit vector, and $\bar{\mathbf{v}} \in \mathbb{C}^{n_r MN \times 1}$ is the noise vector. For antenna selection at the transmitter, pilot symbols can be transmitted from all the n_t antennas and the channel gain of each transmit antenna is estimated at the receiver, and the indices of the transmit antennas to be selected at the transmitter are fed back. Antennas are selected based on the maximum DD channel Frobenius norm, i.e., n_s antennas are selected whose DD channel Frobenius norms, given by

$$\sum_{i=1}^{n_r} \|\mathbf{H}_{ij}\|^2, \quad j = 1, 2, \dots, n_t, \quad (14)$$

are the largest among those of the n_t transmit antennas. Since each \mathbf{H}_{ij} has only PMN non-zero entries with P unique entries, (14) can be equivalently written as

$$\sum_{i=1}^{n_r} \sum_{k=1}^P |h_{ij}^{(k)}|^2, \quad j = 1, 2, \dots, n_t, \quad (15)$$

where $h_{ij}^{(k)}$ are the unique non-zero entries of \mathbf{H}_{ij} . The input-output relation of MIMO-OTFS with TAS can be written as

$$\underbrace{\begin{bmatrix} \mathbf{y}_1 \\ \vdots \\ \mathbf{y}_{n_r} \end{bmatrix}}_{\triangleq \bar{\mathbf{y}}'} = \underbrace{\begin{bmatrix} \mathbf{H}'_{11} & \cdots & \mathbf{H}'_{1n_s} \\ \vdots & \ddots & \vdots \\ \mathbf{H}'_{n_r1} & \cdots & \mathbf{H}'_{n_r n_s} \end{bmatrix}}_{\triangleq \bar{\mathbf{H}}'} \underbrace{\begin{bmatrix} \mathbf{x}_1 \\ \vdots \\ \mathbf{x}_{n_s} \end{bmatrix}}_{\triangleq \bar{\mathbf{x}}'} + \underbrace{\begin{bmatrix} \mathbf{v}_1 \\ \vdots \\ \mathbf{v}_{n_r} \end{bmatrix}}_{\triangleq \bar{\mathbf{v}}'}, \quad (16)$$

or equivalently

$$\bar{\mathbf{y}}' = \bar{\mathbf{H}}'\bar{\mathbf{x}} + \bar{\mathbf{v}}', \quad (17)$$

where $\bar{\mathbf{y}}' \in \mathbb{C}^{n_r MN \times 1}$, $\bar{\mathbf{H}}' \in \mathbb{C}^{n_r MN \times n_s MN}$ is the equivalent channel matrix with TAS, $\bar{\mathbf{x}} \in \mathbb{C}^{n_s MN \times 1}$ is the OTFS transmit vector, and $\bar{\mathbf{v}}' \in \mathbb{C}^{n_r MN \times 1}$ is the noise vector. Figure 2 shows the block diagram of MIMO-OTFS with TAS.

An alternate form of MIMO-OTFS with TAS: Similar to (10), the input-output relation of a MIMO-OTFS with TAS can be written in an alternate form as

$$\underbrace{\begin{bmatrix} \mathbf{y}_1^T \\ \vdots \\ \mathbf{y}_{n_r}^T \end{bmatrix}}_{\triangleq \tilde{\mathbf{Y}}} = \underbrace{\begin{bmatrix} \mathbf{h}'_{11} & \cdots & \mathbf{h}'_{1n_s} \\ \vdots & \ddots & \vdots \\ \mathbf{h}'_{n_r1} & \cdots & \mathbf{h}'_{n_r n_s} \end{bmatrix}}_{\triangleq \tilde{\mathbf{H}}} \underbrace{\begin{bmatrix} \mathbf{X}_1 \\ \vdots \\ \mathbf{X}_{n_s} \end{bmatrix}}_{\triangleq \tilde{\mathbf{X}}} + \underbrace{\begin{bmatrix} \mathbf{v}_1^T \\ \vdots \\ \mathbf{v}_{n_r}^T \end{bmatrix}}_{\triangleq \tilde{\mathbf{V}}}, \quad (18)$$

or equivalently

$$\tilde{\mathbf{Y}} = \tilde{\mathbf{H}}\tilde{\mathbf{X}} + \tilde{\mathbf{V}}, \quad (19)$$

where $\tilde{\mathbf{Y}} \in \mathbb{C}^{n_r \times MN}$ with its i th row corresponding to the received signal in the i th receive antenna, $\tilde{\mathbf{H}} \in \mathbb{C}^{n_r \times n_s P}$ is the channel matrix with $\mathbf{h}'_{ij} \in \mathbb{C}^{1 \times P}$ containing P unique non-zero entries of \mathbf{H}'_{ij} , $\tilde{\mathbf{X}}$ is $n_s P \times MN$ symbol matrix, and $\tilde{\mathbf{V}} \in \mathbb{C}^{n_r \times MN}$ is the noise matrix.

C. OTFS with phase rotation

It has been shown that SISO-OTFS [13] with phase rotation achieves full DD diversity, where the OTFS transmit vector \mathbf{x} is pre-multiplied by a phase rotation matrix Φ , which is of the form

$$\Phi = \text{diag}\{\phi_0, \phi_1, \dots, \phi_{MN-1}\}, \quad (20)$$

where $\phi_i = e^{j a_i}$, $i = 0, 1, \dots, MN - 1$, are transcendental numbers with a_i being real, distinct, and algebraic. That is, $\mathbf{x}' = \Phi \mathbf{x}$ is the phase rotated OTFS transmit vector. For a MIMO-OTFS system, the OTFS vector in each transmit antenna is pre-multiplied by the phase rotation matrix Φ .

D. Rank of MIMO-OTFS systems

In this subsection, we discuss the rank of MIMO-OTFS systems with and without phase rotation.

1) *MIMO-OTFS with $n_s = 1$ with and without phase rotation:* Let $\tilde{\mathbf{X}}_i$ and $\tilde{\mathbf{X}}_j$ be two distinct symbol matrices defined in (19). The minimum rank of $(\tilde{\mathbf{X}}_i - \tilde{\mathbf{X}}_j)$ without phase rotation is $1 < \min(n_s P, MN)$ [13]. Therefore, MIMO-OTFS for $n_s = 1$ and $P > 1$ is rank deficient. For $P = 1$, this system is full rank with rank equal to 1. Next, considering MIMO-OTFS with phase rotation, if $\tilde{\mathbf{X}}'_i$ and $\tilde{\mathbf{X}}'_j$ are the distinct phase rotated symbol matrices in (19) then the minimum rank of $(\tilde{\mathbf{X}}'_i - \tilde{\mathbf{X}}'_j)$ is $P \leq \min(P, MN)$, which is full rank.

2) *MIMO-OTFS with $n_s > 1$ and with and without phase rotation:* For $n_s > 1$, without phase rotation, the minimum rank of $(\tilde{\mathbf{X}}_i - \tilde{\mathbf{X}}_j)$ is $1 < \min(n_s P, MN)$ and with phase rotation the minimum rank is $P < \min(n_s P, MN)$. Both of these cases correspond to rank deficient.

III. DIVERSITY ANALYSIS OF MIMO-OTFS WITH TAS

In this section, we investigate the diversity order of MIMO-OTFS.

A. Full rank MIMO-OTFS systems with TAS

Consider full rank MIMO-OTFS systems with TAS. Let $\tilde{\mathbf{X}}_i$ and $\tilde{\mathbf{X}}_j$ be two distinct symbol matrices and $\gamma = 1/N_0$ be the normalized signal-to-noise ratio (SNR). Assuming perfect DD channel knowledge and maximum likelihood (ML) detection at the receiver, the conditional pairwise error probability (PEP) between symbol matrices $\tilde{\mathbf{X}}_i$ and $\tilde{\mathbf{X}}_j$ is given by

$$P(\tilde{\mathbf{X}}_i \rightarrow \tilde{\mathbf{X}}_j | \tilde{\mathbf{H}}, \tilde{\mathbf{X}}_i) = Q \left(\sqrt{\frac{\|\tilde{\mathbf{H}}(\tilde{\mathbf{X}}_i - \tilde{\mathbf{X}}_j)\|^2}{2N_0}} \right). \quad (21)$$

Averaging over the distribution of $\tilde{\mathbf{H}}$ and upper bounding using the Chernoff bound, the unconditional PEP can be written as

$$P(\tilde{\mathbf{X}}_i \rightarrow \tilde{\mathbf{X}}_j) \leq \mathbb{E}_{\tilde{\mathbf{H}}} \left[\exp \left(-\frac{\gamma \|\tilde{\mathbf{H}}(\tilde{\mathbf{X}}_i - \tilde{\mathbf{X}}_j)\|^2}{4} \right) \right]. \quad (22)$$

The distribution of $\tilde{\mathbf{H}}$ is given by

$$f_{\tilde{\mathbf{H}}}(\mathbf{h}'_1, \dots, \mathbf{h}'_{n_s}) = \frac{n_t!}{(n_t - n_s)!n_s!} \cdot \left(\sum_{l=1}^{n_s} \left[1 - e^{-\|\mathbf{h}'_l\|^2} \sum_{k=0}^{n_r-1} \frac{\|\mathbf{h}'_l\|^{2k}}{k!} \right]^{n_t - n_s} \right) \cdot I_{\tilde{\mathcal{H}}_l}(\mathbf{h}'_1, \dots, \mathbf{h}'_{n_s}), \quad (23)$$

where \mathbf{h}'_i is the i th column of $\tilde{\mathbf{H}}$, $I_{\tilde{\mathcal{H}}_l}(\mathbf{h}'_1, \dots, \mathbf{h}'_{n_s})$ is the indicator function given by

$$I_{\tilde{\mathcal{H}}_l}(\mathbf{h}'_1, \dots, \mathbf{h}'_{n_s}) = \begin{cases} 1 & \text{if } (\mathbf{h}'_1, \dots, \mathbf{h}'_{n_s}) \in \tilde{\mathcal{H}}_l \\ 0 & \text{else,} \end{cases} \quad (24)$$

with non-zero region $\tilde{\mathcal{H}}_l$ where l th column has the minimum norm among the n_s selected columns, i.e., $\tilde{\mathcal{H}}_l =$

$\{\mathbf{h}'_1, \dots, \mathbf{h}'_{n_s} : \|\mathbf{h}'_l\| < \|\mathbf{h}'_k\|, k = 1, \dots, l-1, l+1, \dots, n_s\}$. Using similar steps from [15], the upper bound on PEP can be written as

$$P(\tilde{\mathbf{X}}_i \rightarrow \tilde{\mathbf{X}}_j) \leq \frac{n_t!}{(n_t - n_s)!n_s!(n_r!)^{n_t - n_s}} \cdot \frac{1}{\tilde{\lambda}^{n_t n_r}} \cdot \left(\sum_{i_1=1}^{n_r} \dots \sum_{i_{n_r}(n_t - n_s)=1}^{n_r} k_1! \dots k_{n_r}! \right) \cdot \left(\frac{\gamma}{4} \right)^{-n_r n_t}, \quad (25)$$

where $\tilde{\lambda}$ is the minimum eigenvalue of $(\tilde{\mathbf{X}}_i - \tilde{\mathbf{X}}_j)(\tilde{\mathbf{X}}_i - \tilde{\mathbf{X}}_j)^H$. This result shows that full spatial diversity of $n_t n_r$ is achieved for full rank MIMO-OTFS system when n_s antennas are selected at the transmitter. For $P > 1$, we can predict the diversity order based on the rank of $(\tilde{\mathbf{X}}_i - \tilde{\mathbf{X}}_j)$. We can specialize the above diversity order for MIMO-OTFS systems, which are full rank for $P = 1$ and $P > 1$ as follows.

- MIMO-OTFS system without phase rotation for $P = 1$ is full rank when $n_s = 1$. Therefore, in this case, full spatial diversity of $n_t n_r$ is achieved when one antenna is selected at the transmitter.
- MIMO-OTFS system with phase rotation for $P > 1$ is also full rank when $n_s = 1$. Therefore, in this case, we can predict the diversity order to be $n_r n_t P$ (i.e., full spatial and DD diversity).

B. Rank deficient MIMO-OTFS systems with TAS

Consider rank deficient MIMO-OTFS systems with TAS. Let $\tilde{\mathbf{X}}_i$ and $\tilde{\mathbf{X}}_j$ be two distinct symbol matrices and γ be the normalized SNR. Let r be the minimum rank of $(\tilde{\mathbf{X}}_i - \tilde{\mathbf{X}}_j)$. The upper bound on the PEP can be written as [15]

$$P(\tilde{\mathbf{X}}_i \rightarrow \tilde{\mathbf{X}}_j) \leq \frac{n_t!}{(n_t - n_s)!n_s!(n_r!)^{n_t - n_s}} \cdot \left(\frac{\gamma \tilde{\lambda}}{4} \right)^{-n_r r} \cdot \sum_{i_1=1}^{n_r} \dots \sum_{i_{n_r}(n_t - n_s)=1}^{n_r} \frac{k_1! \dots k_{n_r}!}{(1 + \frac{\gamma \tilde{\lambda}}{4})^{k_1+1} \dots (1 + \frac{\gamma \tilde{\lambda}}{4})^{k_{n_r}+1}}, \quad (26)$$

where $\tilde{\lambda}$ is the minimum non-zero eigenvalue of $(\tilde{\mathbf{X}}_i - \tilde{\mathbf{X}}_j)(\tilde{\mathbf{X}}_i - \tilde{\mathbf{X}}_j)^H$. From the above equation, the diversity achieved for the rank deficient case is at least $r n_r$. For any $P > 1$, we can predict the diversity order based on the minimum rank of symbol difference matrices. Now, we can specialize in the above result to MIMO-OTFS systems that are rank deficient as follows.

- MIMO-OTFS without phase rotation for $P = 1$ is rank deficient when $n_s > 1$, with minimum rank of one. Therefore, only n_r th order diversity is achieved.
- MIMO-OTFS without phase rotation is rank deficient for $P > 1$ and $n_s \geq 1$, with minimum rank equal to one. Therefore, predicted diversity order in this case, is n_r .
- MIMO-OTFS with phase rotation is also rank deficient for $P > 1$ and $n_s > 1$, with minimum rank equal to P . Therefore, predicted diversity order in this case is $n_r P$.

| Parameter | Value |
|--|---|
| Carrier frequency, f_c (GHz) | 4 |
| Subcarrier spacing, Δf (KHz) | 3.75 |
| Frame size (M, N) | (2, 2) |
| DD profile for $P = 1$ (τ_i (μ s), ν_i (kHz)) | $(\frac{1}{M\Delta f}, \frac{1}{NT})$ |
| DD profile for $P = 2$ (τ_i (μ s), ν_i (kHz)) | $(0, 0), (\frac{1}{M\Delta f}, \frac{1}{NT})$ |
| Maximum speed (km/h) | 506.2 |
| Modulation scheme | BPSK |

TABLE I: Simulation parameters.

IV. RESULTS AND DISCUSSIONS

In this section, we discuss the bit error rate (BER) performance of TAS with and without phase rotation for MISO-OTFS and MIMO-OTFS systems for $P = 1, 2$ and $n_s = 1, 2$. The simulation parameters used are tabulated in Table I.

MISO/MIMO-OTFS with TAS for $P = 1, n_s = 1, 2$ without phase rotation: Figure 3 shows the simulated BER performance of MISO-OTFS and MIMO-OTFS without phase rotation for $P = 1, n_r = 1, 2, n_s = 1, 2$, and $n_t = 2, 3$. All the systems use OTFS frame size of $M = N = 2$, and BPSK modulation with ML detection at the receiver. A carrier frequency of 4 GHz and subcarrier spacing of 3.75 kHz with maximum Doppler of 1.875 kHz (corresponding speed is 506.2 km/h at 4 GHz) are considered. The DD channel model considered for simulations is as per (8), and the various DD profiles used are given in Table I. For MISO-OTFS system with $P = 1$ and $n_s = 1$ the system is full ranked and the analytically derived diversity in Sec. III-A is n_t . From Fig. 3 it is evident that diversity slopes of 2 and 3 are observed for the MISO-OTFS systems with $n_t = 2, n_s = 1$ and $n_t = 3, n_s = 1$, respectively, corroborating the analytically predicted diversity order. For MIMO-OTFS system with TAS with $P = 1, n_r = 2, n_t = 3$, and $n_s = 2$, the system is rank deficient with rank equal to 1 and analytically predicted diversity order is n_r . The BER plot in Fig. 3 shows a diversity slope of 2 for this system, verifying the analytical predicted diversity order in Sec. III-B.

MISO/MIMO-OTFS with TAS for $P = 2$ and $n_s = 1, 2$ with and without phase rotation: Figure 4 shows upper bound and the simulated BER performance of 1) MISO-OTFS with TAS, without phase rotation for $P = 2, n_t = 2$, and $n_s = 1$ and 2) MIMO-OTFS with TAS, without and with phase rotation for $P = 2, n_t = 3, n_s = 2$, and $n_r = 2$. The parameters for simulations are given in Table I. The upper bound is based on the union bound for the considered system. The considered system is rank deficient and predicted diversity in Sec. III-B is rn_r . Figure 4 shows diversity slopes of 1 for MISO-OTFS without phase rotation, 2 and 4 for MIMO-OTFS without and with phase rotation, respectively. For the considered MISO-OTFS and MIMO-OTFS system, the rank is 1 for without phase rotation, and 2 for MIMO-OTFS system with phase rotation. Also, the upper bound on BER is tight at high SNRs for all the cases, verifying the predicted diversity of rn_r in Sec. III-B.

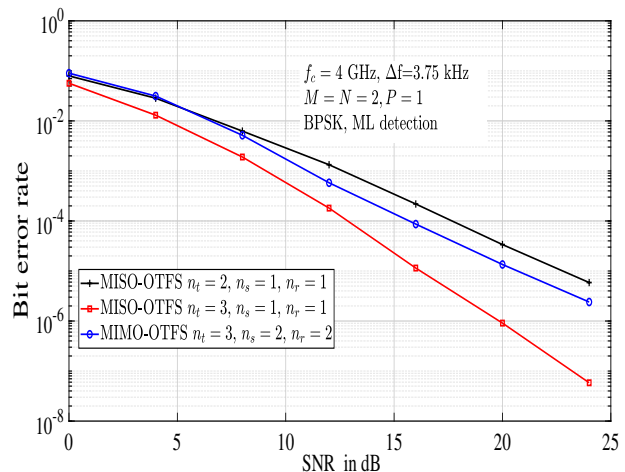


Fig. 3: BER performance of MISO/MIMO-OTFS with TAS, without phase rotation for $P = 1, n_r = 1, 2, n_s = 1, 2$, and $n_t = 2, 3$.

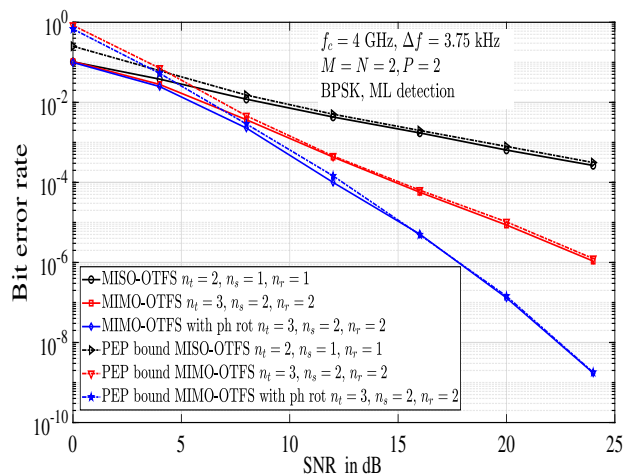


Fig. 4: BER performance of MISO/MIMO-OTFS with TAS, without and with phase rotation for $P = 2, n_t = 2, 3, n_s = 1, 2$ and $n_r = 1, 2$.

Comparison between Frobenius norm based selection, random selection, and no selection: Figure 5 compares the BER performance with Frobenius norm based antenna selection, random antenna selection, and without antenna selection in OTFS systems with phase rotation and $P = 2$. In random selection, n_s distinct antennas are selected at random. The systems considered in Fig. 5 are: SISO-OTFS without selection ($n_t = n_r = 1$), MISO-OTFS with Frobenius norm based selection and random selection ($n_t = 2, n_s = 1, n_r = 1$), MIMO-OTFS without selection ($n_t = n_r = 2$), and MIMO-OTFS with Frobenius norm based selection and random selection ($n_t = 2, n_s = 1, n_r = 2$). It is noted that, as per the analysis in Sec. III, the considered SISO-OTFS system without selection and MISO-OTFS and MIMO-OTFS systems with Frobenius norm based selection ($n_s = 1$) are full rank, and hence they achieve the full diversity of $n_t n_r P$. That is,

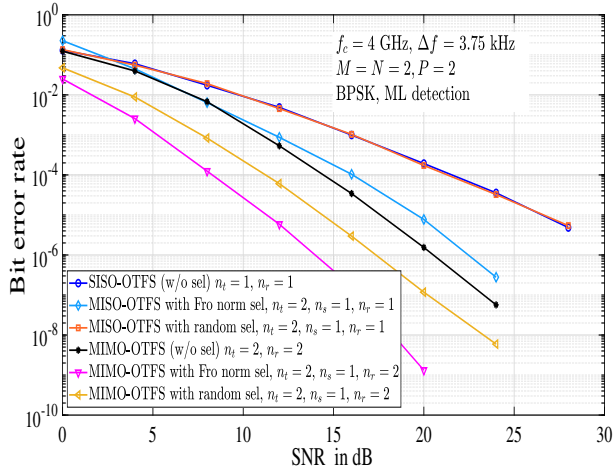


Fig. 5: BER performance comparison between *i*) Frobenius norm based selection, *ii*) random selection, and *iii*) no selection in OTFS systems with phase rotation and $P = 2$.

SISO-OTFS has a diversity of $n_t n_r P = 2$, and MISO-OTFS and MIMO-OTFS with norm based selection have a diversity of $n_t n_r P = 4$ and $n_t n_r P = 8$, respectively. These diversity slopes of 2, 4, and 8 can be observed in the corresponding BER plots of SISO-OTFS, MISO-OTFS with norm based selection, and MIMO-OTFS with norm based selection, respectively, in Fig. 5. Likewise, the considered MIMO-OTFS system without selection is rank deficient and it achieves a diversity of $n_r P = 4$. It is also seen that MISO-OTFS with random selection ($n_s = 1$) does not give diversity slope improvement compared to without selection. MIMO-OTFS with random selection ($n_s = 1$) gives some SNR gain compared to MIMO-OTFS without selection but has the same diversity slope of 4, whereas the norm based selection achieves a diversity slope of 8. Other selection criteria, such as capacity based selection criteria, can be considered for further investigation.

V. CONCLUSIONS

We investigated the diversity performance of OTFS modulation with antenna selection at the transmitter. The receiver was assumed to know the DD channel and send limited feedback to the transmitter. Antenna selection was made based on the maximum channel Frobenius norms in the DD domain. We quantified the diversity orders of the MIMO-OTFS with TAS for full rank and rank deficient cases for $P = 1$. Our analysis showed that MIMO-OTFS with TAS for $P = 1$ achieves full spatial diversity of $n_r n_t$ when $n_s = 1$ due to full rank, and only n_r -th order diversity is achieved when $n_s > 1$ due to rank deficiency. Simulation results on the BER performance validated the analytically predicted diversity orders. For $P > 1$, diversity orders were predicted through the rank of symbol difference matrices, validated through computation of PEP bounds and simulations. Diversity analysis of TAS for $P > 1$, fractional DD values, and practical pulse shapes at the transmitter and receiver, can be considered for future work.

Also, capacity based antenna selection in OTFS can also a potential topic for future work.

REFERENCES

- [1] R. Hadani, S. Rakib, M. Tsatsanis, A. Monk, A. J. Goldsmith, A. F. Molisch, and R. Calderbank, "Orthogonal time frequency space modulation," *Proc. IEEE WCNC'2017*, pp. 1-7, Mar. 2017.
- [2] R. Hadani, S. Rakib, S. Kons, M. Tsatsanis, A. Monk, C. Ibars, J. Delfeld, Y. Hebron, A. J. Goldsmith, A. F. Molisch, and R. Calderbank, "Orthogonal time frequency space modulation," online: arXiv:1808.00519v1 [cs.IT] 1 Aug 2018.
- [3] P. Raviteja, K. T. Phan, and Y. Hong, "Embedded pilot-aided channel estimation for OTFS in delay-Doppler channels," *IEEE Trans. Veh. Tech.*, vol. 68, no. 5, pp. 4906-4917, May 2019.
- [4] Rasheed O K, G. D. Surabhi, and A. Chockalingam, "Sparse delay-Doppler channel estimation in rapidly time-varying channels for multiuser OTFS on the uplink," *Proc. IEEE VTC'2020-Spring*, May 2020.
- [5] P. Raviteja, K. T. Phan, Y. Hong, and E. Viterbo, "Interference cancellation and iterative detection for orthogonal time frequency space modulation," *IEEE Trans. Wireless Commun.*, vol. 17, no. 10, pp. 6501-6515, Aug. 2018.
- [6] M. K. Ramachandran and A. Chockalingam, "MIMO-OTFS in high-Doppler fading channels: signal detection and channel estimation," *Proc. IEEE GLOBECOM'2018*, Dec. 2018.
- [7] G. D. Surabhi and A. Chockalingam, "Low-complexity linear equalization for OTFS modulation," *IEEE Commun. Letters*, vol. 24, no. 2, pp. 330-334, Feb. 2020.
- [8] V. Khammammetti and S. K. Mohammed, "OTFS based multiple-access in high Doppler and delay spread wireless channels," *IEEE Trans. Wireless Commun.* vol. 8, no. 2, pp. 528-531, Apr. 2019.
- [9] R. M. Augustine and A. Chockalingam, "Interleaved time-frequency multiple access using OTFS modulation," *Proc. IEEE VTC'2019-Fall*, Sep. 2019.
- [10] Z. Ding, R. Schober, P. Fan, and H. V. Poor, "OTFS-NOMA: an efficient approach for exploiting heterogeneous user mobility profiles," *IEEE Trans. Commun.*, vol. 67, no. 11, pp. 7950-7965, Nov. 2019.
- [11] G. D. Surabhi, R. M. Augustine, and A. Chockalingam, "Peak-to-average power ratio of OTFS modulation," *IEEE Commun. Letters*, vol. 23, no. 6, pp. 999-1002, Jun. 2019.
- [12] P. Raviteja, Y. Hong, E. Viterbo, and E. Biglieri, "Practical pulse shaping waveforms for reduced-cyclic-prefix OTFS," *IEEE Trans. Veh. Tech.*, vol. 68, no. 1, pp. 957-961, Jan. 2019.
- [13] G. D. Surabhi, R. M. Augustine, and A. Chockalingam, "On the diversity of uncoded OTFS modulation in doubly-dispersive channels," *IEEE Trans. Wireless Commun.*, vol. 18, no. 6, pp. 3049-3063, Jun. 2019.
- [14] R. M. Augustine, G. D. Surabhi, and A. Chockalingam, "Space-time coded OTFS modulation in high-Doppler channels," *Proc. IEEE VTC'2019-Spring*, pp. 1-6, 2019.
- [15] T. Gucluoglu, T. M. Duman, "Performance analysis of transmit and receive antenna selection over flat fading channels," *IEEE Trans. Wireless Commun.*, vol. 7, no. 8, pp. 3056-3065, Aug. 2008.